Applied Catalysis B: Environmental 199 (2016) 315–322

Contents lists available at ScienceDirect

Applied Catalysis B: Environmental

journal homepage: www.elsevier.com/locate/apcatb

Synthesis of novel visible light response $Ag_{10}Si_4O_{13}$ photocatalyst

Xianglin Zhu [a], Peng Wang [a,*], Baibiao Huang [a,*], Xiangchao Ma [b], Xiaoyan Qin [a], Xiaoyang Zhang [a], Ying Dai [b]

[a] State Key Laboratory of Crystal Materials, Shandong University, Jinan 250100, China
[b] School of Physics, Shandong University, Jinan 250100, China

ARTICLE INFO

Article history:
Received 1 April 2016
Received in revised form 12 June 2016
Accepted 18 June 2016
Available online 23 June 2016

Keywords:
Novel visble photocatalyst
$Ag_{10}Si_4O_{13}$
High photocatalytic activity
Moderate and facial method
Reactive species of photocatalysts

ABSTRACT

In this work, a novel photocatalyst $Ag_{10}Si_4O_{13}$ was synthesized through a facile solid state reaction. The as prepared $Ag_{10}Si_4O_{13}$ was characterized by XRD, SEM, TEM, UV–vis and XPS. The photocatalytic capability of $Ag_{10}Si_4O_{13}$ was estimated through photo-degradation of MB solution and photocatalytic oxygen generation under visible light irradiation. TOC changes of MB solution before and after photocatalytic experiment identified the mineralization of MB molecules. During photocatalytic oxygen generation reaction, Co_3O_4 was used as cocatalyst to boost oxygen evolution. Compared with pure $Ag_{10}Si_4O_{13}$, 4% $Co_3O_4/Ag_{10}Si_4O_{13}$ showed higher efficiency in oxygen evolution. Radical-trapping experiments and results show that holes generated by $Ag_{10}Si_4O_{13}$ are main active ingredient-oxidizing organic pollution under light irradiation.

1. Introduction

Social development depends on modern industry a lot. Large amount of fossil energy has been consumed to keep high development rate of world economy. Energy shortage of fossil fuel and environment problem hamper the development of society. Seeking for inexhaustible and green energy is highly desirable in the past decades. As the environmental pollution and energy shortage become more and more severe, solar energy as a kind of completely natural and clean energy source catches a lot of attention. Photocatalysis technique shows promising application prospect in solving these problems for its ability of decomposing organic pollutants, water splitting by using solar energy [1–8]. However, the low photocatalytic efficiencies of existing catalysts fail to meet the requirements of industrialization and commercialization, greatly limiting the further development of photocatalysis. So it is urgent to explore new photocatalysts with high efficiencies.

Among various found photocatalysts, Ag-based photocatalyst shows high photocatalytic efficiency and has been proved to be one of the most attractive candidates, which works under visible light irradiation. According to the past reports, the visible light photocatalytic ability of Ag-based photocatalysts can be attributed from two aspects: Localized surface plasmon resonance effects (LSPRs) coming from the silver nanoparticles deposited on semiconductor and visible light response owing to the nature properties of photocatalysts. As for some photocatalysts with wide band gap, visible light cannot be used directly, only after depositing silver nanoparticles, these photocatalysts can absorb visible light and show visible light photocatalytic activities. This is because silver nanoparticles can absorb visible light and be excited to generate electrons and holes, joining in further photocatalytic reaction [9–12], just like Ag/AgCl, Ag/TiO_2 materials etc. For others, the materials can absorb visible light because of their proper band gaps and show photocatalytic activity under irradiation of visible light [13–17]. Ye and her group have synthesized Ag_3PO_4 through a co-precipitation method and their experiment showed that Ag_3PO_4 was a very good photooxidation catalyst in photodegradation of organic pollutants. The excellent performance of Ag_3PO_4 photocatalyst sets off the upsurge of Ag based visible light photocatalysts.

Silicate is famous for its great variety and variable compositions, but only a few of silicate photocatalysts were studied [18–21]. In the researched silicate photocatalysts, silver silicate showed good visible light response and should be attractive candidates. Tae-Gon Kim etc. have reported the photocatalytic property of $Ag_9(SiO_4)_2NO_3$ [18], and proved that unique d10 electronic configurations of Ag^+ ions can take part in the composition and hybridization of the energy band in the Ag-based compounds, which is beneficial to adjust the band gap and light absorption properties of materials. This point makes $Ag_9(SiO_4)_2NO_3$ show excellent visible light photocatalytic activity in oxygen evolution and organic dye

* Corresponding authors.
E-mail addresses: pengwangicm@sdu.edu.cn (P. Wang), bbhuang@sdu.edu.cn (B. Huang).

http://dx.doi.org/10.1016/j.apcatb.2016.06.048
0926-3373/

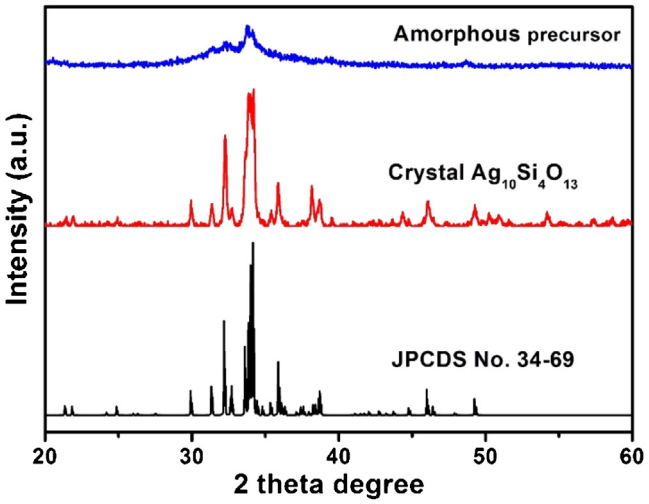

Fig. 1. XRD patterns of as-prepared samples (For interpretation of the references to colour in the text, the reader is referred to the web version of this article.)

decomposition. Recently, our group reported the novel $Ag_6Si_2O_7$ semiconductor as a visible-light-responsive photocatalyst showed significantly high activity in photocatalytic reduction of Cr^{6+} and oxidization of MB. As for the high efficiency of $Ag_6Si_2O_7$ photocatalyst, the built-in polarized electric field caused by its special crystal structure plays a key role on separation of photogenerated carriers, besides, d10 electronic configurations of Ag^+ ions are benefit to the visible light absorption [21]. Inspired by the former work, $Ag_{10}Si_4O_{13}$ containing d10 electronic configurations of Ag^+ ions should be another promising visible light photocatalyst. Insofar we can see, there is no report on photocatalytic properties of $Ag_{10}Si_4O_{13}$. In tradition, synthesis of $Ag_{10}Si_4O_{13}$ was at a condition of high oxygen pressure of ca. 4.5 kbar and 600 °C [22]. The harsh synthetic condition is an obstacle to its application in photocatalyst. In this paper, $Ag_{10}Si_4O_{13}$ was synthesized through a moderate and facial method, used as visible light photocatalyst to oxide water and degrade MB. This special synthetic route may provide reference for synthesizing other silver silicate which are hard to synthesis at mild reaction conditions.

2. Experimental details

2.1. Synthesis of $Ag_{10}Si_4O_{13}$

$Ag_{10}Si_4O_{13}$ was synthesized through a two-step method. Firstly, $AgNO_3$ and $Na_2SiO_3{\cdot}9H_2O$ with molar ratio of 3:1 were mixed and ground for 20 min until the mixture showed uniform color. Then the mixture was transferred into glass beaker, and 100 mL deionized water were added. After 10 min stirring and the precipitation were separated and dried at air temperature. Amorphous precursor was got. Secondly, $Ag_{10}Si_4O_{13}$ with good crystallinity was got through a quenching method. In detail, the dried precipitation was transferred to an alumina crucible and heated to 400 °C for 4 h at a rate of 5 °C per minute. After the crucible was cooled down to room temperature, the mixture was ground for later use. Co_3O_4 was loaded by a thermal decomposition method [23], typically 500 mg $Ag_{10}Si_4O_3$ precursor powder and 25 mg $Co(NO_3)_2{\cdot}6H_2O$ were added into 1 mL aqueous solution containing 0.5 mL deionized water and ethyl alcohol. The mixture was ground until got dried, then the dried powder was heated according the method we got crystal $Ag_{10}Si_4O_3$. Finally, the 4% (mass fraction) $Co_3O_4/Ag_{10}Si_4O_3$ catalyst was obtained. The N-doped TiO_2 was prepared by nitridation of commercially available Degussa P25 powder at 773 K for 10 h under NH_3 flow (flow rate of 350 mL min^{-1}) [9].

2.2. Characterization

The structure of $Ag_{10}Si_4O_{13}$ was characterized by X-ray diffraction (XRD) on a Bruker AXS D8 advance powder diffractometer (Cu Kα X-ray radiation, λ = 0.154056 nm). The morphologies of as-prepared samples were obtained using scanning electron microscopy (SEM, Hitachi S4800). UV–vis diffuse reflectance spectra were obtained for the dry-pressed disk samples by using a Shimadzu UV 2550 recording spectrophotometer, which was equipped with an integrating sphere and $BaSO_4$ was used as a reference. The visible light source was obtained from a 300 W Xe arc lamp (PLS-SXE 300, Beijing Trusttech Co. Ltd.) equipped with an ultraviolet cutoff filter. (λ > 420 nm) The amount of O_2 produced was determined by a gas chromatograph (Varian GC-3800) equipped with thermal conductivity detector.

2.3. Photocatalytic experiments

The photocatalytic performances of $Ag_{10}Si_4O_{13}$ were evaluated by discoloration of MB dye solution and photocatalytic water splitting experiments under visible light irradiation (λ > 420 nm). In a typical run, 50 mg $Ag_{10}Si_4O_{13}$ was dispersed in 50 mL MB dye solution (20 mg/L). The mixed suspension was firstly put in dark for 20 min to establish adsorption-desorption equilibrium. Then, it was put under 300 W Xe arc lamp equipped with a UV cutoff filter (λ > 420 nm). 5 mL of the mixed suspension was taken every 10 min and centrifuged to remove the powders. The residual concentration of organic dye solutions were determined by measuring the maximum absorption with a UV–vis spectrophotometer. Photocatalytic production of oxygen was carried out in presence of $AgNO_3$. Typically, 100 mg photocatalyst was added into 100 mL of aqueous $AgNO_3$ solution (0.015 M), which was kept at 10 °C in a quartz reactor. The reactor was sealed and vacuumed in order to drive away the residual oxygen and switched on the 300 W Xe lamp. The output of oxygen was detected at 2.5 h. Photo-electrochemical measurements were carried out in 0.1 M Na_2SO_4 solution at potential of 0.9 V (vs. RHE)

3. Results and discussion

The XRD patterns of as-prepared samples are shown in Fig. 1. Blue line is XRD of amorphous precursor. Red line is XRD of crystal $Ag_{10}Si_4O_{13}$. Black line is standard card. As seen from XRD result, sample with good crystallinity was got after quenched at 400 °C for 4 h, all peaks of the as-prepared sample can be indexed to the triclinic $Ag_{10}Si_4O_{13}$ (JCPDS No. 34-69). There were no redundant peaks occurring in the XRD patterns, indicating that the prepared sample was pure $Ag_{10}Si_4O_{13}$ material.

The morphologies of as-prepared samples were characterized by scanning electron microscopy and transmission electron microscopy as shown in Fig. 2. Particle sizes of $Ag_{10}Si_4O_{13}$ are estimated to be around 1–2 μm. Due to the synthesis method, no uniform morphologies was got in our experiment. The morphologies of Co_3O_4 loaded $Ag_{10}Si_4O_{13}$ were almost the same as $Ag_{10}Si_4O_{13}$ particles'. The morphologies are the typical one made from solid-phase sintering method. As remarkable cocatalyst, the dispersal of Co_3O_4 on $Ag_{10}Si_4O_{13}$ was key factor to determine the photocatalytic efficiency in oxygen evolution. So it's important to identify whether Co_3O_4 was uniform dispersed in the catalyst. As shown in Fig. 2c–f, Co_3O_4 was homogeneously loaded on the surface of $Ag_{10}Si_4O_{13}$. This is good for photocatalytic oxygen evolution.

The color of the as-prepared samples is salmon pink, expected to be able to absorb visible light. The diffused reflectance spectra is shown in Fig. 3, the as-prepared samples exhibit strong

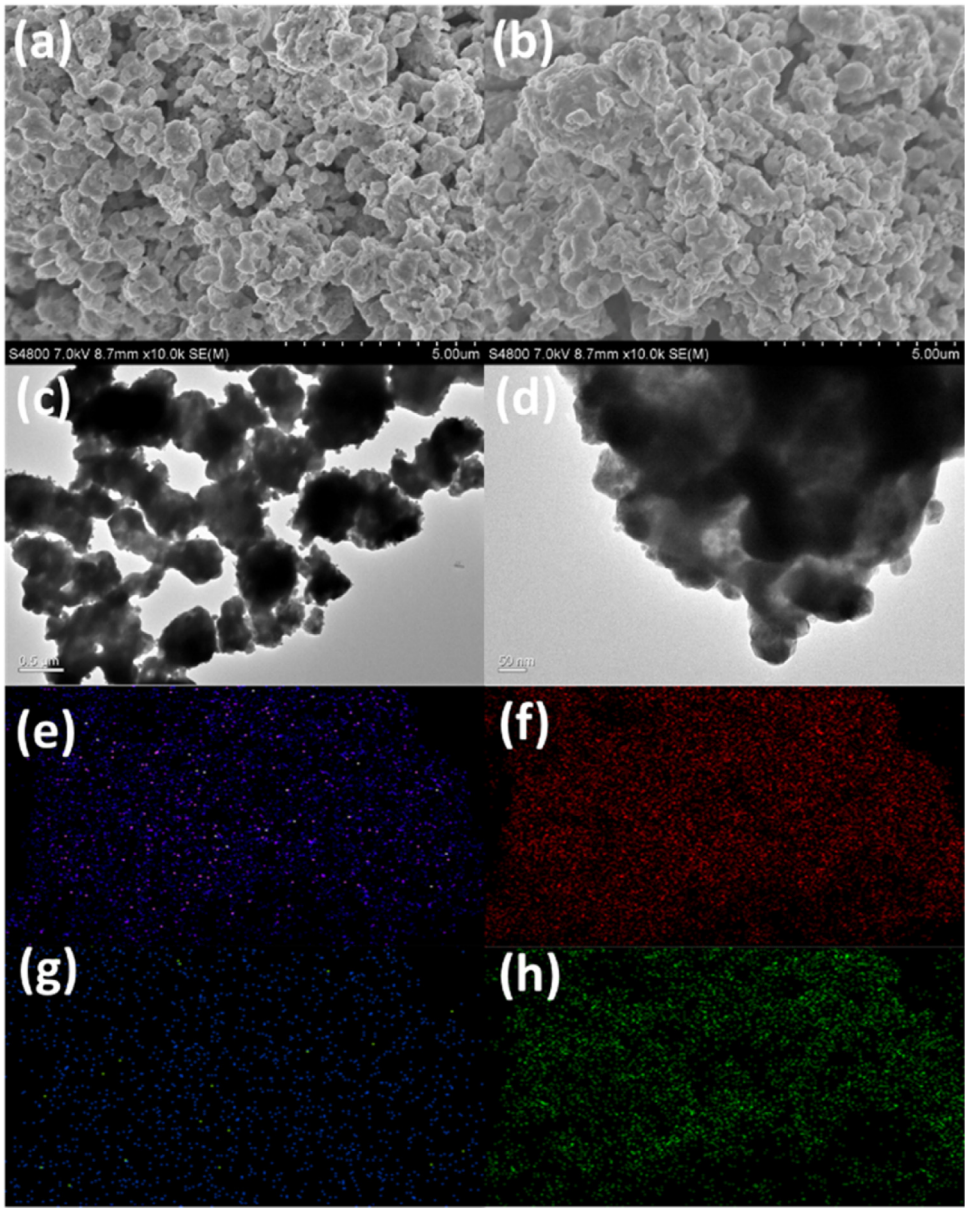

Fig. 2. (a) SEM image of $Ag_{10}Si_4O_{13}$, (b) SEM image of 4% $Co_3O_4/Ag_{10}Si_4O_{13}$, (c–d) TEM images of 4% $Co_3O_4/Ag_{10}Si_4O_{13}$, (e–f) mapping results of 4% $Co_3O_4/Ag_{10}Si_4O_{13}$, (e–h) responding to Ag,Si,Co and O element.

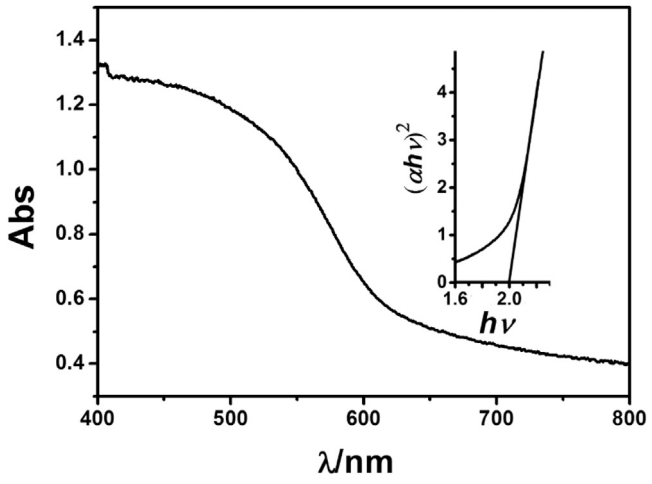

Fig. 3. Diffused reflectance spectra, the inset is the $(\alpha h\nu)^2$ vs. $h\nu$ plot.

light absorption in visible-light region. According to the $(\alpha h\nu)^2$ vs. $h\nu$ plot shown in the inset of Fig. 3, the estimated band gap of as-prepared $Ag_{10}Si_4O_{13}$ is about 2.0 eV. The conduction band (CB) and valence band (VB) positions of $Ag_{10}Si_4O_{13}$ were estimated following the empirical equation: $E_{VB} = \chi\text{-}E^e + 0.5E_g$, where E_{VB} is the valence band-edge potential, χ is the electronegativity of the semiconductor, expressed as the geometric mean of the absolute electronegativity of the constituent atoms, E^e is the energy of free electrons on the hydrogen scale (4.5 eV *vs.* NHE), E_g is the band gap energy of the semiconductor. Calculations method about the CB and VB was according to our previous work [24,25]. And the estimated CB and VB band edge of $Ag_{10}Si_4O_{13}$ is 0.34 eV and 2.34 eV vs. NHE. Compared with O_2/H_2O (1.23 eV), $Ag_{10}Si_4O_{13}$ can be used as a good oxidative photocatalysts to produce O_2.

In order to evaluate photocatalytic activities of as-prepared samples. Photo-degradation of organic dye solutions and photocatalytic O_2 production experiments were carried out. Fig. 4a is the

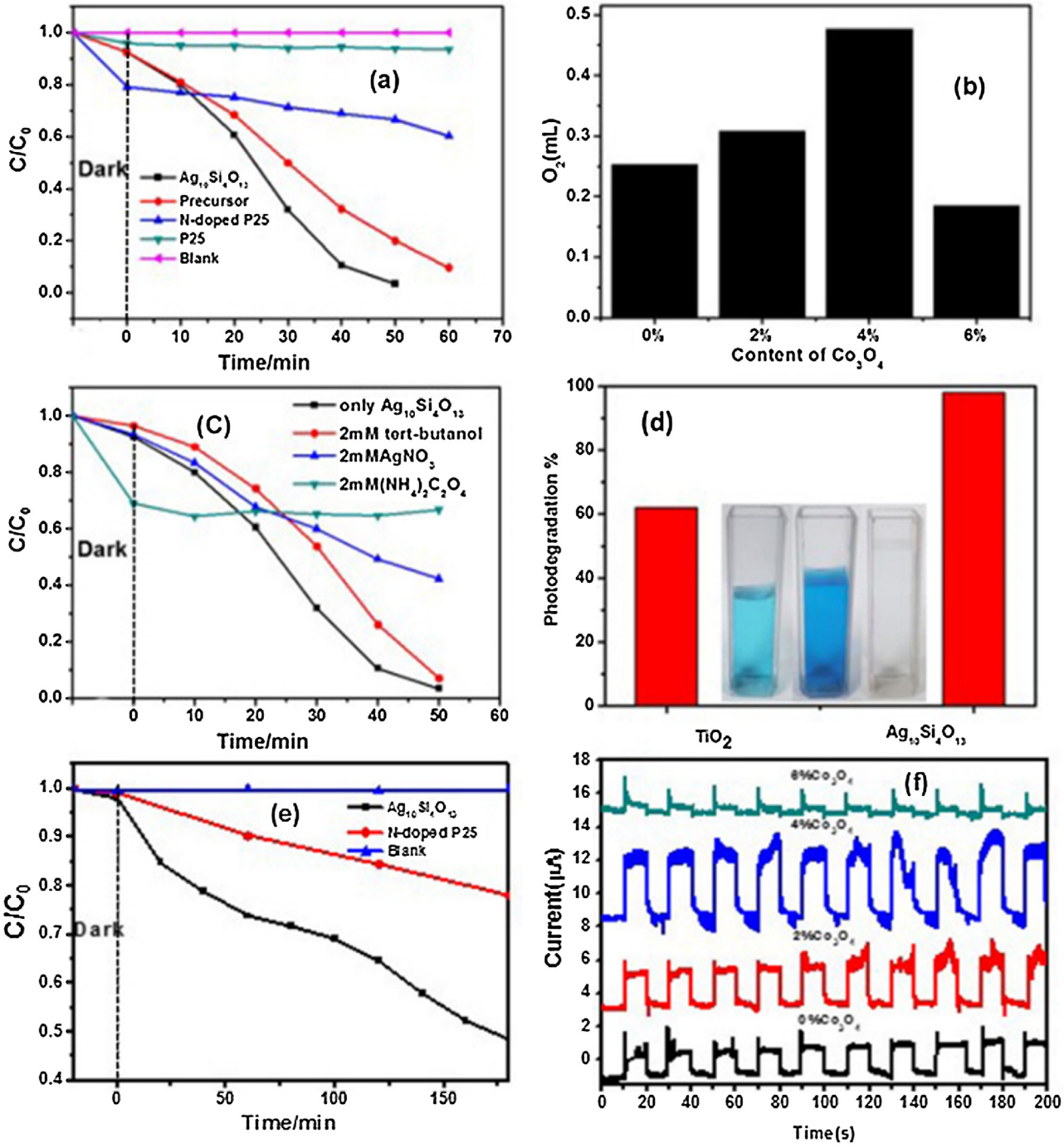

Fig. 4. (a) Photo-degradation of MB dye solutions under visible light irradiation (λ > 420 nm), (b) Photocatalytic O_2 production from water under visible light irradiation (λ > 420 nm), (c) Photocatalytic experiment in presence of ammonium oxalate, $AgNO_3$, *tert*-butanol respectively under visible light irradiation (λ > 420 nm), (d) Photo-degradation of MB dye solutions at 7 min under UV–vis light (300nm–1100 nm), The photo on the left is result of TiO_2, the middle is initial MB, the right is result of $Ag_{10}Si_4O_{13}$, (e) Photo-degradation phenol under visible light irradiation (λ > 420 nm), (f) Photo-electrochemical results of $Ag_{10}Si_4O_{13}$ with different content of Co_3O_4 (λ > 420 nm).

result of photo-degradation of organic dyes (MB) and Fig. 4b is O_2 production (in presence of $AgNO_3$) under visible light irradiation (λ > 420 nm). From the results we can see, both amorphous precursor and crystal $Ag_{10}Si_4O_{13}$ had photocatalytic activities, crystal $Ag_{10}Si_4O_{13}$ showed better performance in MB photo-degradation. As for crystal $Ag_{10}Si_4O_{13}$, nearly 98% MB dye was degraded in 50 min. Compared to N-doped P25 and pure P25, both crystal $Ag_{10}Si_4O_{13}$ and amorphous precursor showed better photocatalytic activities under visible light irradiation. The efficiency of photocatalyst is usually limited by electron–hole recombination, meanwhile the loading of cocatalyst is a practicable way to prevent electron–hole recombination. Fig. 4b is the results of photocatalytic O_2 production experiment in 2.5 h with doping different amount of Co_3O_4. After loading Co_3O_4 (4 wt%), the volume of generated O_2 was about 0.5 mL, which was 2 times higher than that of pure $Ag_{10}Si_4O_{13}$. The presence of Co_3O_4 promoted the separation of photo-induced carrier and enhanced the efficiency of water oxidation. Photocatalytic oxidation activity was also characterized

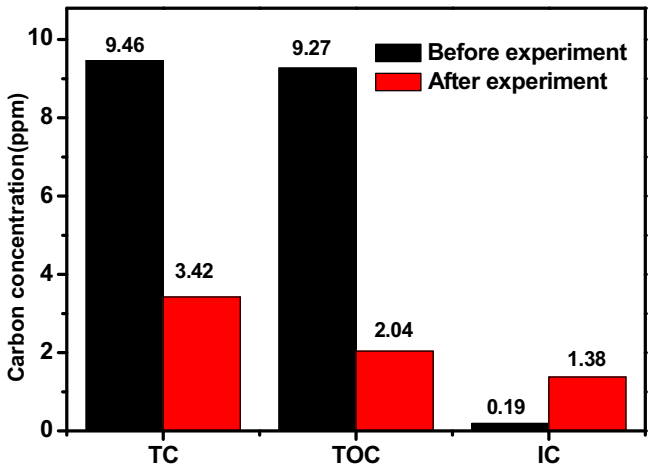

Fig. 5. Carbon concentration during the photocatalytic experiments. TC is total carbon, TOC is total organic carbon and IC is inorganic carbon.

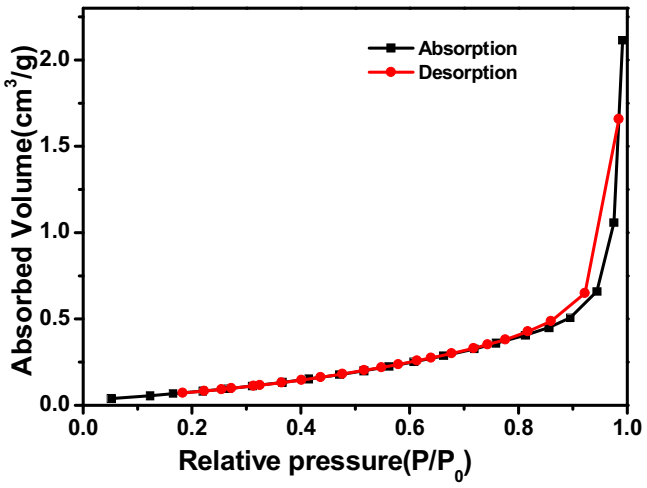

Fig. 6. Nitrogen adsorption–desorption isotherms.

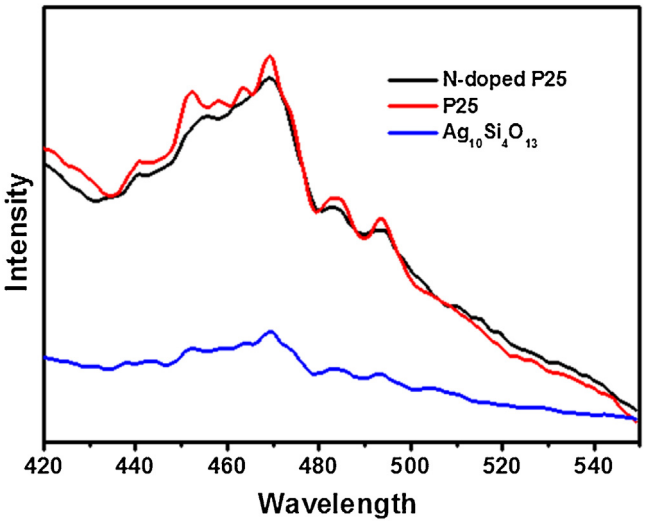

Fig. 7. Photoluminescence spectra of the photocatalysts.

under UV–vis light (300 nm–1100 nm) just as shown in Fig. 4(d), only in 7 min over 98% MB dye was removed by $Ag_{10}Si_4O_{13}$, meanwhile only 62% MB dye was removed by P25 in the same time. Photo-degradation of phenol was also carried out under visible light irradiation and the result showed that both $Ag_{10}Si_4O_{13}$ and N-dpoed P25 could photodegrade phenol, while $Ag_{10}Si_4O_{13}$ had better activity. In order to prove the enhanced charge separation between Co_3O_4 and $Ag_{10}Si_4O_{13}$, photo-electrochemical experiment [26–30] was carried out. Just as shown in Fig. 4(f), 4% $Co_3O_4/Ag_{10}Si_4O_{13}$ had the best photo-electrochemical property, indicating the best charge separation, which is in accord with the water oxidation experiment. Based on these results $Ag_{10}Si_4O_{13}$ was proved to be a high efficient photocatalyst under visible light and full spectrum light.

In general, the major reactive species of photocatalysts have three kinds (hole, •OH radical and superoxide radical) during the photocatalytic degradation of organic dye [31]. The active ingredients of $Ag_{10}Si_4O_{13}$ photocatalyst were studied by radical-trapping experiments employing ammonium oxalate (a hole scavenger), $AgNO_3$ (an electron scavenger) and *tert*-butanol (an •OH radical scavenger) under identical conditions. As shown in Fig. 4c, the overall degradation rate slightly changes in presence of *tert*-butanol, indicating that •OH radical is not the main active ingredient. When $AgNO_3$ was added, the degradation rate got slowly especially after 20 min of reaction, this may be caused by mass metal silver deposited on photocatalyst and this showed photogenerated electrons did not work in the photocatalytic progress. When ammonium oxalate was added, the adsorption of MB was enhanced but the concentration of MB solution didn't reduce under the irradiation of visible light. These results indicated that the photogenerated holes are the major reactive species during MB degradation.

In the progress of pollutants discoloration, it is very important to determine whether the organic pollutants are mineralized to inorganic CO_2 or other carbonate. In order to confirm the mineralization of organic pollution, total carbon (TC), total organic carbon (TOC) and inorganic carbon (IC) was measured during the photo-degradation process. Seen from Fig. 5, the TOC and IC of original MB solution was 9.27 ppm and 0.189 ppm. After photo-degradation progress, TOC and IC were 2.043 ppm and 1.377 ppm, respectively. TOC of MB solution significantly decreased, about 78% of organic dye molecules was mineralized, and only small part of organic species was left in the solution according to our TOC measurement.

As photocatalytic reaction is an interfacial catalysis progress, specific surface area is important for the activity. The surface area of as-prepared sample was determined by nitrogen physical adsorption–desorption method. Seen from Fig. 6, the BET surface area is only about 0.36 m^2/g, much smaller than that of P25 (about 50 m^2/g), demonstrating that BET surface area plays only a small part in the activity of $Ag_{10}Si_4O_{13}$ in our work. We think that photocatalytic activity of $Ag_{10}Si_4O_{13}$ may be further improved by preparing sample with bigger BET surface area.

As a useful technique to explore the separation efficiency of photo-generated electrons and holes, photoluminescence (PL) analysis is widely used. PL emission of photocatalyst mainly results from the recombination of charge carriers. Typically, lower PL intensity means better separation efficiency of photo induced electron-hole pairs, and it is benefit to the photocatalytic activity. Fig. 7 is the PL spectra of N-doped P25, P25 and $Ag_{10}Si_4O_{13}$ under the excitation wavelength of 300 nm at room temperature. From the results, it can be seen that $Ag_{10}Si_4O_{13}$ shows weakest PL intensity, indicating $Ag_{10}Si_4O_{13}$ has best charge carriers separation efficency.

To further confirm the valence state of $Ag_{10}Si_4O_{13}$ composite, XPS measurements were employed to analyze. Fig. 8d is the full XPS survey scan of $Ag_{10}Si_4O_{13}$ composite which exhibits the characteristic peaks of C 1s, Ag 3d, Si 2p and O 1s. The high resolution XPS patterns of Ag 3d, Si 2p and O 1 s are shown in Fig. 8a–c. Two peaks at 267.53 eV and 373.53 eV respond to characteristic peaks of

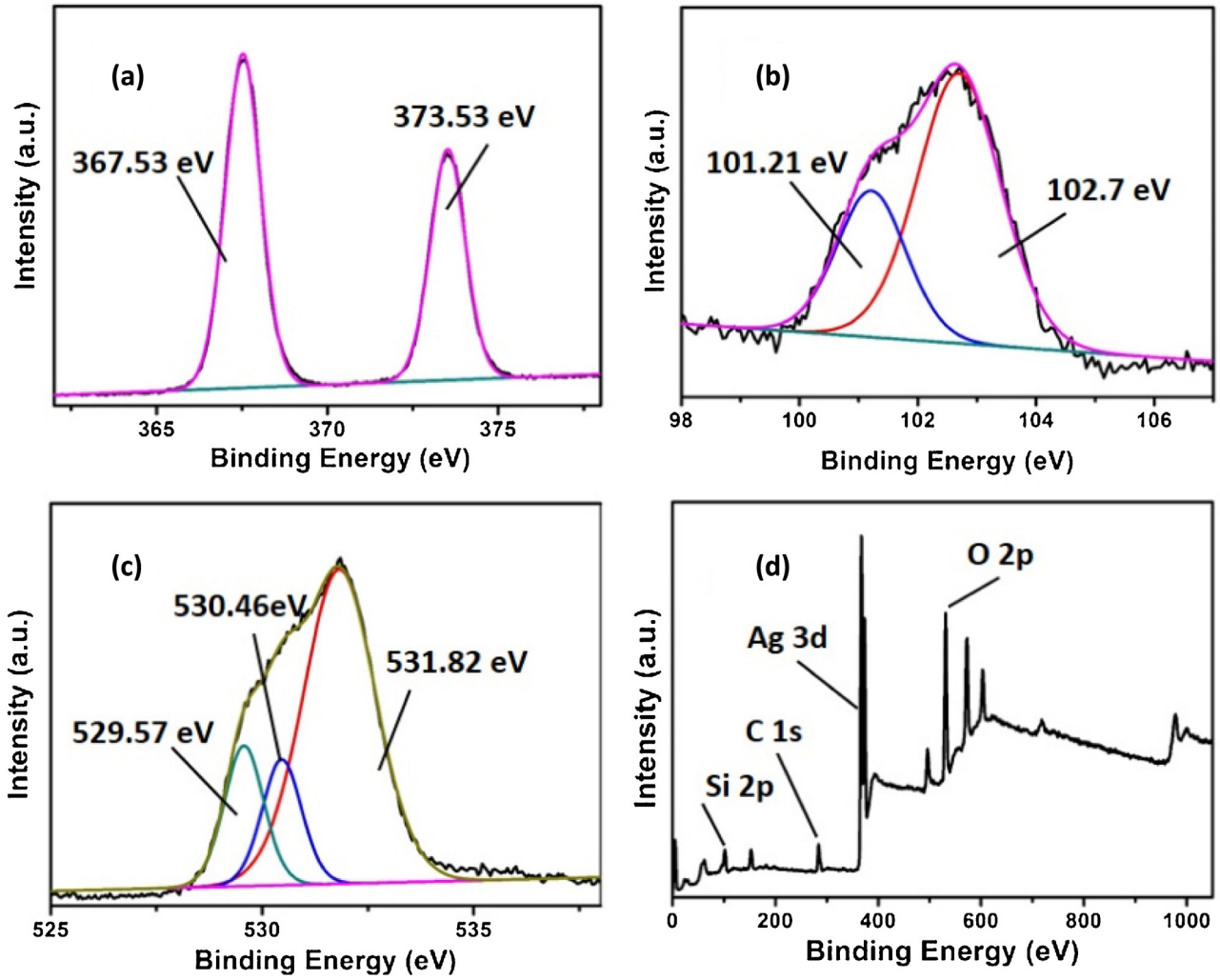

Fig. 8. XPS spectra of the samples.

Ag^+ in $Ag_{10}Si_4O_{13}$ [32], no obvious Ag^0 is found in the XPS test. This proves that the visible light absorption and photocatalytic activity is not coming from LSPRs. Peaks at 101.21 eV and 102.7 eV are the characteristic peaks of Si 2p. Three peaks at about 529.57 eV, 530.46 eV and 531.82 eV are signals of O1s [33].

So as to fully understand the photocatalytic mechanism of $Ag_{10}Si_4O_{13}$, first-principles calculations based on density functional theory (DFT) were used to estimate the density of states. Fig. 9a is the down spin energy band structures of $Ag_{10}Si_4O_{13}$, from the result we can get a conclusion that $Ag_{10}Si_4O_{13}$ is a direct band gap semiconductor. Fig. 9b–d give the calculation results of gap states. Fig. 9b is the total density of states (TDOS) for the s and p states. Fig. 9c and d are constitute states of CB and VB. In the $Ag_{10}Si_4O_{13}$ crystal, the edge of CB is main composed of Ag 3d and O2p states, the edge of VB is main constituted of Ag s and O 2p states. Calculations results show that Ag plays an important role on the constitution of CB and VB, and this is consistent with the early reports that d10 electronic configurations of Ag^+ ions are benefit to the visible light absorption.

Based on all the experiment results, we propose the possible mechanism (as shown in Fig. 10) to explain the visible light photocatalytic activity of as prepared photocatalyst. $Ag_{10}Si_4O_{13}$ has band gap of 2.0 eV and it can be excited by the visible light. Photo generated electrons and holes will occur when catalyst absorbs visible light. The VB of $Ag_{10}Si_4O_{13}$ is about 2.34 eV and the generated holes have enough oxidizing ability to oxidize organic dyes to CO_2 and oxidize H_2O to generate O_2. As a result, the color of MB solution fades and O_2 is generated under the irradiating of light when $Ag_{10}Si_4O_{13}$ is added.

4. Conclusion

In summary, a novel Ag-based photocatalyst $Ag_{10}Si_4O_{13}$ has been synthesized through a simple method. The photocatalytic activities of as prepared samples were characterized by photo-degradation of MB solution and photocatalytic O_2 evolution. Experiment results show that $Ag_{10}Si_4O_{13}$ has visible light photocatalytic activity both in photo-degradation of MB and photocatalytic O_2 generation. The addition of cocatalyst Co_3O_4 plays a significant role in oxygen evolution, and it can improve the efficiency of photocatalyst obviously. The possible mechanism was also discussed and photo generated holes as the major reactive species occurred when the photocatalyst was under irradiating of visible light. The low cost and abundance of silicates make $Ag_{10}Si_4O_{13}$ a good candidate for environmental improvement and solar energy conversion.

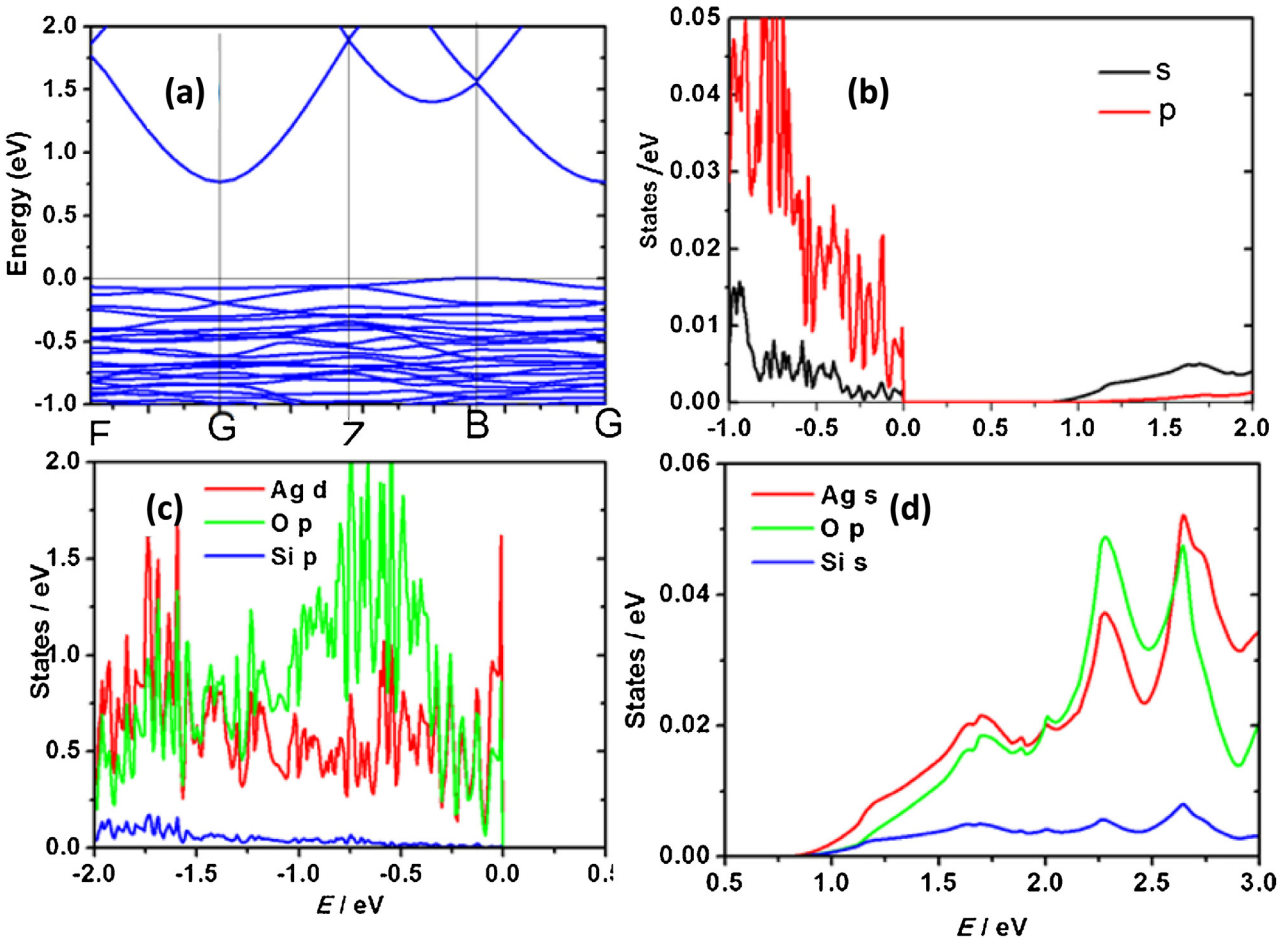

Fig. 9. Electronic structure of $Ag_{10}Si_4O_{13}$ calculated by DFT.

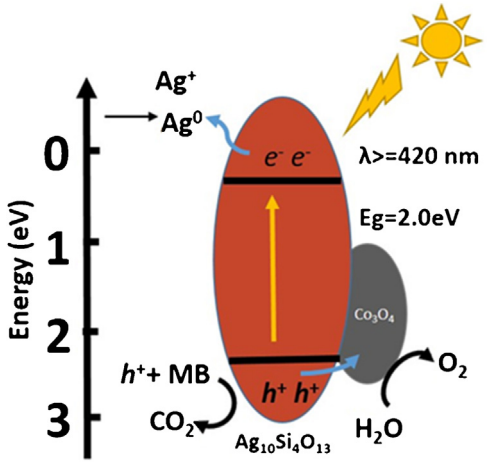

Fig. 10. Schematic photocatalytic reaction process of $Ag_{10}Si_4O_{13}$ catalyst.

Acknowledgements

This work was financially supported by a research Grant from the National Basic Research Program of China (973 progarm, No. 2013CB632401), the National Natural Science Foundation of China (No. 21333006, 21573135, 11374190, 51002091, and 21007031), The Recruitment Program of Global Experts, China, Taishan Scholar Foundation of Shandong Province, China, and Shandong Province Natural Science Foundation (ZR2014JL008).

Notes and references

[1] Akira Fujishima, kenichi Honda, Nature 238 (1972) 37–38.
[2] Xiaobo Chen, Shaohua Shen, Liejin Guo, Samuel S. Mao, Chem. Rev. 110 (2010) 6503–6570.
[3] Jeongsuk Seo, Tsuyoshi Takata, Mamiko Nakabayashi, Takashi Hisatomi, Naoya Shibata, Tsutomu Minegishi, Kazunari Domen, J. Am. Chem. Soc. 137 (2015) 12780–12783.
[4] Tae Hwa Jeon, Wonyong Choi, Hyunwong Park, Phys. Chem. Chem. Phys. 13 (2011) 21392–21401.
[5] Wenjie Shan, Yun Hu, Zhaogao Bai, Mengmeng Zheng, Chaohai Wei, Appl. Catal. B: Environ. 188 (2016) 1–12.
[6] Li Liu, Yuehong Qi, Jinshan Hu, Weijia An, Shuanglong Lin, Yinghua Liang, Wenquan Cui, Mater. Lett. 158 (2015) 278–281.
[7] Xiang Lan, Junying Zhang, Hong Gao, Tianmin Wang, CrystEngComm 13 (2011) 633–636.
[8] Li Liu, Yuehong Qi, Jinrong Lu, Shuanglong Lin, Weijia An, Yinghua Liang, Wenquan Cui, Appl. Catal. B: Environ. 183 (2016) 133–141.
[9] Peng Wang, Baibiao Huang, Xiaoyan Qin, Xiaoyang Zhang, Ying Dai, Jiyong Wei, Myung-Hwan Whangbo, Angew. Chem. Int. Ed. 47 (2008) 7931–7933.
[10] Koichi Awazu, Makoto Fujimaki, Carsten Rockstuhl, Junji Tominaga, Hirotaka Murakami, Yoshimichi Ohki, Naoya Yoshida, Toshiya Watanabe, J. Am. Chem. Soc. 130 (2008) 1676–1680.
[11] Zhiyuan Chen, Liang Fang, Wen Dong, Fengang Zheng, Mingrong Shen, Junling Wang, J. Mater. Chem. A 2 (2014) 824–832.
[12] Yanyuan Wen, Hanming Ding, Yongkui Shan, Nanoscale 3 (2011) 4411–4417.
[13] Peng Wang, Baibiao Huang, Xiaoyang Zhang, Xiaoyan Qin, Hao Jin, Ying Dai, Zeyan Wang, Jiyong Wei, Jie Zhan, Shaoying Wang, Junpeng Wang, Myung-Hwan Whangbo, Chem. Eur. J. 15 (2009) 1821–1824.
[14] Xuefei Wang, Shufen Li, Huogen Yu, Jiaguo Yu, Shengwei Liu, Chem. Eur. J. 17 (2011) 7777–7780.
[15] Jianting Tang, Yonghong Liu, Haizhu Li, Zhen Tan, Datang Li, Chem. Commun. 49 (2013) 5498–5500.
[16] Zhiguo Yi, Jinhua Ye, Naoki Kikugawa, Tetsuya Kako, Shuxin Ouyang, Hilary Stuart-Williams, Hui Yang, Junyu Cao, Wenjun Luo, Zhaosheng Li, Yun Liu, Ray L. Withers, Nat. Mater. 9 (7) (2010) 559–564.

[17] Hongjun Dong, Gang Chen, Jingxue Sun, Chunmei Li, Yaoguang Yu, Dahong Chen, Appl. Catal. B: Environ. 134-135 (2013) 46–54.
[18] Tae-Gon Kim, Dong-Hee Yeon, Taehyung Kim, Jeonghee Lee, Seoung-Jae Im, Appl. Phys. Lett. 103 (2013) 043904.
[19] Xiaolei Liu, Wenjun Wang, Yuanyuan Liu, Baibiao Huang, Ying Dai, Xiaoyan Qin, Xiaoyang Zhang, RSC Adv. 5 (2015) 55957–55963.
[20] Peiyang Zhang, Juncheng Hu, Jinlin Li, RSC Adv. 1 (2011) 1072–1077.
[21] Zaizhu Lou, Baibiao Huang, Zeyan Wang, Xiangchao Ma, Rui Zhang, Xiaoyang Zhang, Xiaoyan Qin, Ying Dai, Myung-Hwan Whangbo, Chem. Mater. 26 (2014) 3873–3875.
[22] Martin Jansen, Hans-Lothar Keller, Angew. Chem. Int. Ed. Engl. 18 (6) (1979).
[23] Jiarui Wang, Frank E. Osterloh, J. Mater. Chem. A 2 (2014) 9405–9411.
[24] Xianglin Zhu, Zeyan Wang, Baibiao Huang, Wei Wei, Ying Dai, Xiaoyang Zhang, Xiaoyan Qin, APL Mater. 3 (2015) 104413.
[25] Rui Zhang, Ying Dai, Zaizhu Lou, Yanmei Yang, Xiaoyan Qin, Xiaoyang Zhang, Baibiao Huang, CrystEngComm (16) (2014) 4931–4934.
[26] Wenquan Cui, Yanfei Liu, Li Liu, Jinshan Hu, Yinghua Liang, Appl. Catal. A: Gen. 417 (2012) 111–118.
[27] Wenquan Cui, Huan Wang, Li Liu, Yinghua Liang, Joanne Gamage McEvoy, Appl. Surf. Sci. 283 (2013) 820–827.
[28] Yinghua Liang, Shuanglong Lin, Li Liu, Jinshan Hu, Wenquan Cui, Appl. Catal. B Environ. 164 (2015) 192–203.
[29] Shouwei Zhang, Jiaxing Li, Xiangke Wang, Yongshun Huang, Meiyi Zeng, Jinzhang Xu, Appl. Surf. Sci. 283 (2013) 820–827.
[30] Hui Zhang, Xinfei Fan, Xie Quan, Shuo Chen, Hongtao Yu, Environ. Sci. Technol. 45 (13) (2011) 5731–5736.
[31] Haiping Li, Jingyi Liu, Wanguo Hou, Na Du, Renjie Zhang, Xutang Tao, Appl. Catal. B: Environ. 160–161 (2014) 89–97.
[32] Hideyuki Katsumata, Takahiro Hayashi, Masanao Taniguchi, Tohru Suzuki, Satoshi Kaneco, Mater. Res. Bull. 63 (2015) 116–122.
[33] Sojin Kim, Chanhoi Kim, Jin-Yong Hong, Sun Hye Hwang, Jyongsik Jang, RSC Adv. 4 (2014) 6821–6824.